Investigation of the Stability and Electronic Structures for Exohedral Al_n Doped (Mono and Double)-Layer MgO Nanosheet s: A DFT Approach

Nibras Mossa Umran[1], Haneen Ali Rashed[2], Aseel Mustafa Abdul Majeed[3], Gagandeep Kaur[4]

[1,2] Department of Physics, College of Science, University of Kerbala, Karbala, Iraq

[3] Department of Physics, College of Science, University of Mustansiryah University, Baghdad, Iraq

[4] Department of Applied Sciences, Chandigarh Group of Colleges-College of Engineering, Landran, Mohali, Punjab, India

Email: [1]nibrasmossa@uokerbala.edu.iq

ABSTRACT

In present work, a detailed analysis of density functional theory (DFT) study performed on pure and doped MgO nanosheet(MgONs). The aim of this work is to explore the stability skeleton, and electronic properties of mono layer of the MgO nanosheets and analogous double-layers with various positions of exohedral Al_n dopant atoms. Our results for pure and doped MgO nanosheet corroborate with previous theoretical and experimental data. Optimized structures of monolayer and analogous double-layers of MgO nanosheet (MgONs) result in stable 2-D configuration, especially on doping with large concentrations. It has been observed that the band gap decreases with the increase in concentration of doping while the electronegativity increases.

Keywords

DFT, MgO nanosheet, exohedral doped, electronegativity, hardness

Article Received: XX Xxx 2021, Revised: XX Xxx 2021, Accepted: XX Xxx 2021

Introduction

Nanomaterials have attracted a great interest for theoretical and experimental research due to their unique physical and chemical characteristics which depend on the shape and size of nanomaterials, like hardness with high conductivit, [1, 2]. One of the important nanomaterial is Magnesium oxide, which is a famous simple oxide with rock salt structure in bulk phase. The 2D-MgO with both polar (111) and nonpolar (001) orientations have been successfully grown on various substrates experimentally [3-10]. This leads to the possibility of changing the electronic structure through doping which has recognized as a favorable alleyway to tune the properties of oxide materials toward the demands of different physics and chemistry applications. Dopants are supposed to disturb the lattice structure locally by breaking bonds to nearby atoms. As a consequence, interatomic coupling gets [11]. Density functional theory (DFT) study for electronic calculations of MgO mono-layer have also shown to display a more fascinating feature than its bulk phase for instance shrinking the band gap from 7.8 eV to 3.1 eV (for GGA) and 4.2 eV (for GGA-mBJ) [12]. The DFT calculations of Cr doped Rocksalt MgO reveal that CrMg3O4 is a promising spintronic material due to its half-metallic ferromagnet property as well as its resistivity to deform due to the large bulk modulus and shear modulus [13].

Fascinated by the interesting properties of doped MGO NSs, we perform density functional theory (DFT) to examine the stable structure, and electronic properties (binding energy, ionization potential, electron affinity, electronegativity and hardness) of hexagonal MgO NSs (111) after exohedral doping by Al_n. Three geometries i.e mono layer of MgO NSs in first and second case, and two layers of MgONs in the third case have been considered for investigation.

Computational Approach

Ab initio calculations in this study have been performed using the Spanish initiative for electronic simulations with thousands of atoms (SIESTA) program package [14, 15] which implements density functional theory (DFT) using exchange correlation functional of generalized gradient approximation (GGA) [16,17] and utilizing the double zeta basis (DZ) to exhibit spin polarization [18]. The pseudo-potential standards are built by using Trouiller- Martins schemes which are described as the interaction of valence electrons with atomic central. Pseudopotentials with $2s^2\ 2p^6\ 3s^2$ and $3s^2\ 3p^1$ valence electron configurations were used for Mg, O, and Al

atoms, respectively. Conjugate gradient (CG) algorithm is used to get optimized structures of MgO NSs. The positions of all atoms are allowed to fully relax until the force on each atom is less than 0.008 eV/Å during relaxation. The energy cut-off of 200Ry has been used to define the finite real space grid for numerical integrals.

Results and Discussion

3.1 Doping of Al_n(n=1-7) on single layered MgO NS:

We start by investigating a pure MgO NSs by optimizing it with the atomic structure focused along either the (100) or (111) direction.The lattice constant for the optimized MgO NSs(100) and the MgO NSs (111) obtained were 3.85 and 3.18 Å respectively which are in good agreement with the previous results (4.01 and 3.26 Å)[19-22]. Also, the resulting Mg−O bond length of optimized pure MgO (111) NSs comes out to be 1.99 Å with bond angles between Mg-O-Mg bonds equal to 120^o which is comparable to formerly obtained results [7,21] as shown in **Fig.1**. Further on comparing the binding energies of both structures, it was found that, the binding energy of the optimized MgONs(111) system decreases by about 0.28 eV per Mg−O pair, which indicates that this MgONs(111) is more stable than the MgONs(100).

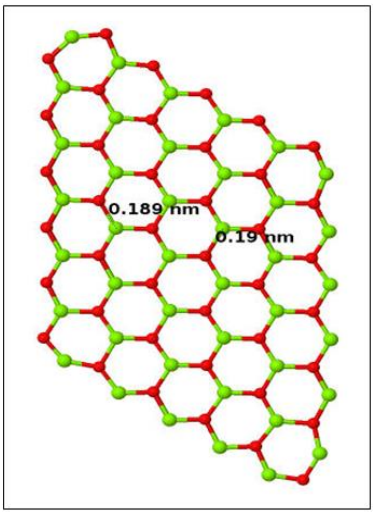

Fig.1: Optimize structure of MgO NSs pure, the green and red spheres refer to Magnesium and Oxygen atoms respectively.

After optimization of the pure hexagonal MgO NSs, we perform a full geometry optimization of Al_n (n=1-6) exohedral doped MgO NSs. The atomic configurations for the Al doped MgO NSs are shown in **Fig.2**. The bond length obtained between the dopant Al and it nearest Mg atom (Al-Mg distance) is 2.6 Å, while Al-O bond length comes out to be 2.38 Å[23]. Also, we observe that the dopant Al atom is still in the same plane as the Mg and O atoms causing strain into the lattice of the MgO NSs.

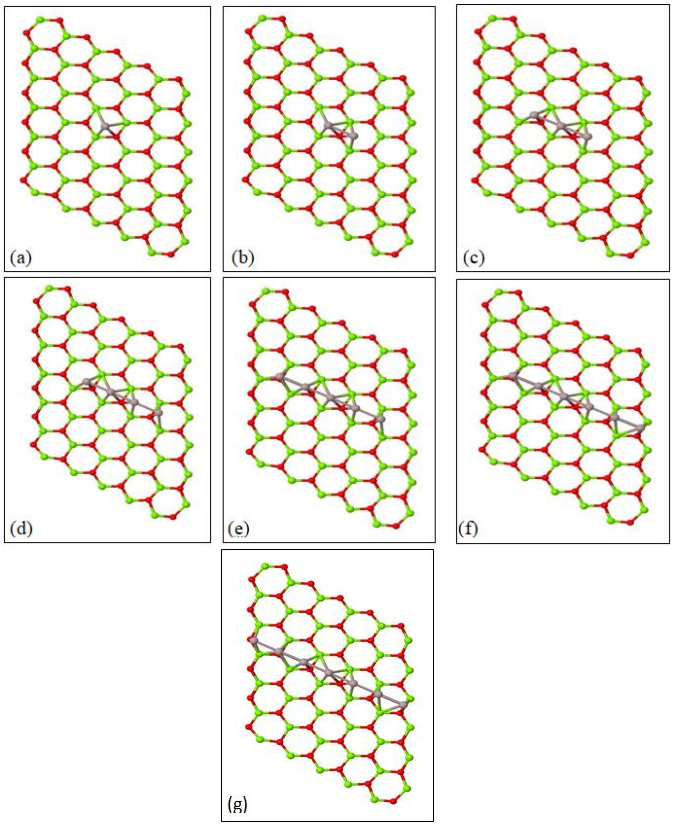

Fig.2(a-g): Optimize structure of Al_n (n= 1-7), the green, red, and gray spheres refer to magnesium, oxygen, and the aluminum dopant atoms respectively.

Figure 2: For the optimized doped structures , the binding energy per atom (E_b) of the doped systems has been calculated to evaluate their stability by using the equation[19]:

$$E_b = \left(E_{mMgO} - E_{MgO} - nE_m\right)/N \quad (1)$$

Where, E_{mMgO}, and E_{MgO} are total energies of the Al doped MgONs and the pristine MgO NS, respectively, while n represent the number of dopant, E_m total energy of the Al dopant and N is the total number of atoms in a supercell (n=82). A negative value of binding energy corresponds to a metastable or stable bound dopant when both are present in the system[22]. The variation of binding energy per atom for doped MgO NS is

shown in **Fig.3**. It is clear from Fig. 3 that with the increase in the number of Al dopants, the binding energy of the MgO NS attains its maximum value at -17.4 eV for Al_7. The binding energy oscillates for Al_4 for Al_6 dopants. From the structural analysis, it is found that the stability of MgO NS strongly depends upon the number of dopant atoms in the sheet.

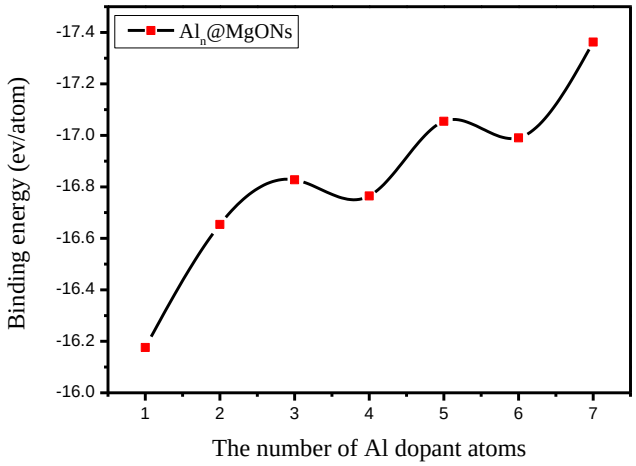

Fig.3: Binding energy per atom of variation Al_n@MgO NS with a number of dopants (n=1-7).

The energy gaps of Al_n@MgO NS are lesser than that of the related MgO NS and they depend on the type of dopant, number of dopants as shown in **Fig.4**. The band gaps for Al_n@MgO NS were calculated from highest occupied molecular orbital (HOMO) and the lowest unoccupied molecular orbital (LUMO) play a very important role[24]. The gap between HOMO and LUMO energy levels can be used to measure the kinetic stability of system under consideration. Larger the HOMO-LUMO gap, Larger will be the kinetic stability as it is energetically not favorable to add electrons to a high lying LUMO or to remove electrons from a low-lying HOMO.

Further, we notice that the doping with Al_4, Al_5, and Al_7 are found to decrease the bandgaps of the MgO NS with increase the number of dopant. It is observed that the increase of the bandgap of the MgO with the decrease of the number of dopant[25]. This indicates that as the number of dopant increases, calculations show that all cases of Al_n@MgO NS display semiconducting behavior and the Al_n@MgO NS becomes energetically favorable.

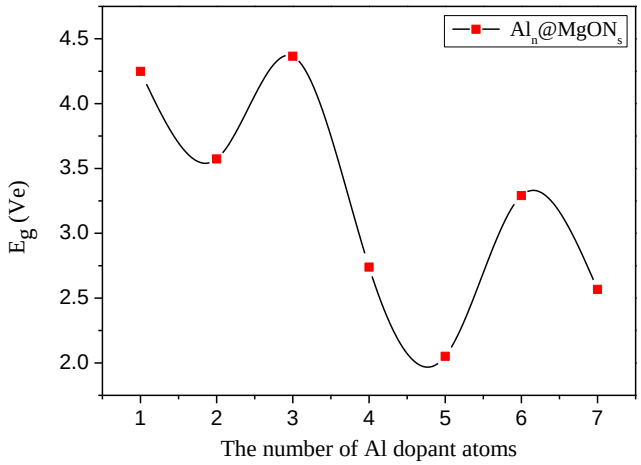

Fig.4: The band gaps of Al_n@MgO NS (n=1-7) in eV.

We have calculated the ionization potential (IP) by making nanosheet of Al_n@MgO one electron deficient. Total energy for Al_n@MgO NS complex is computed and then the total energy of neutral Al_n@MgO NS is subtracted from it [26]. In the similar manner, electron affinity (EA) is calculated by putting one extra electron in neutral Al_n@MgO NS and computing the total energy for the same and then subtracting the total energy of neutral Al_n@MgO NS (n=1-7) [26,27]. It is clear that, exohedral doping of MgO NS effects EA more than that of IP. IP is independent on the postion of the atom, but in case of n=7 the structure has higher IP, as illustrated in **Fig.5**. While the calculated EA of the studied structures is of the order of n=1-7. At the same time, this structure has the higher value of electron affinity EA. It is clear from the graphs shown in figure 5 that the MgO NS doped with Al atoms have higher values of IP and EA than that of the original MgO NS. That means, these structures have high ability to accept electrons and become anions in comparison with MgO NS. However, they cannot easily donate an electron to the surrounding species.

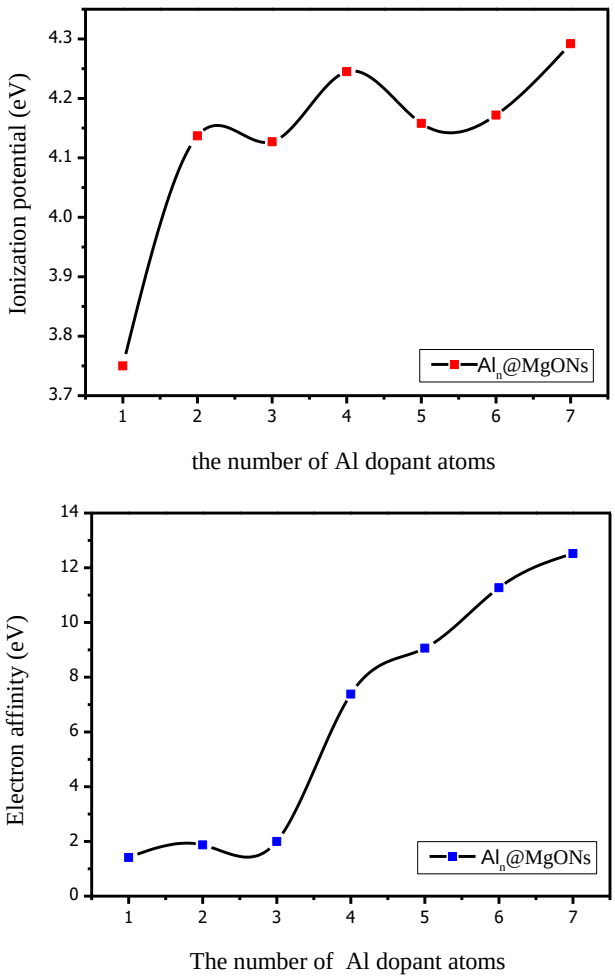

Fig.5: (a) The ionization potential and (b) electron affinity of Al_n@MgONs (n=1-7) in eV.

Next, we obtain the electronegativity (EN) which is a linear combination of two known physical quantities i.e. ionization energy and electron affinity and is expressed as [20]:

$$EN = (IP + EA) / 2 \quad (2)$$

As discussed, the hardness (H) is defined in terms of ionizations energies and electron affinities, the hardness is half of the energy gap between two frontier orbitals [27]:

$$H = IP - EA \quad (3)$$

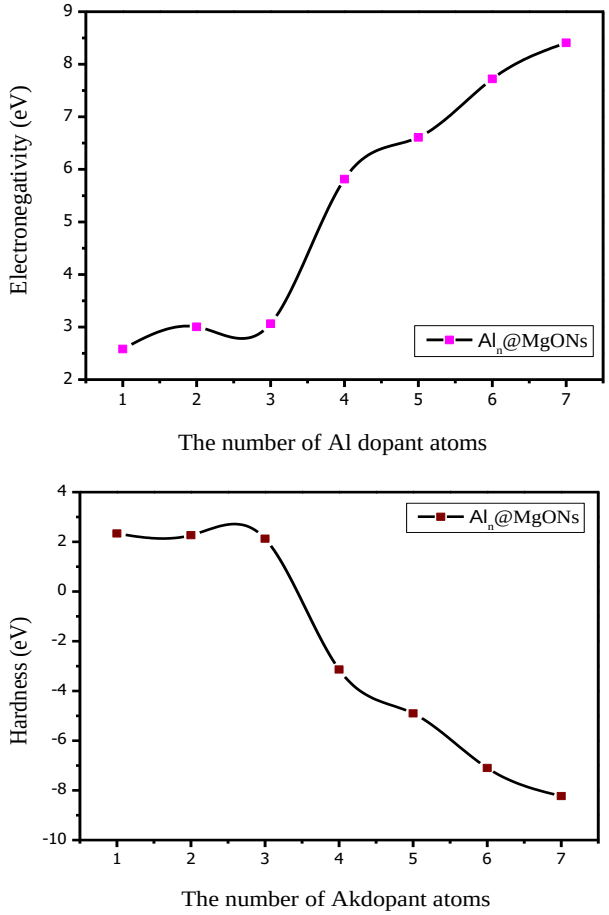

Fig.6: (a) The electronegativity and (b) hardness of Al_n@MgO NS(n=1-7) in eV.

According to **Fig. 6(a)**, the behavior of the electronegativity (EN) is shown for Al exohedral doped in $MgON_S$. One can see that the addition of Al dopant atoms in $MgON_S$ leads to increase in the EN of the $MgON_S$, this may come from the variation in the electronegativity of Mg atoms (1.3eV) and O atoms (3.5eV). The influence of the hardness H is illustrated in **Fig. 6(b)**. Except the Al_7MgO NS structure, all the other structures have higher values of H which means except Al_7MgO NS, all other structures are more soft.

3.2 Doping of Al_{14}, Al_{28} and Al_{35} on single layered MgONs:

As minor variations in the lattice parameters might suggest high solubility of Al in MgO NS, it refers to the extent of the impact the Al dopants on the MgO NS (and vice versa). The structural geometries of Al_n@MgO NS (n=14, 28, and 35) are collected in **Fig. 7**. Whereas adopted equal the distance between lines of $Al_{7\text{-}35}$ exohedral doped This means that Al_{28} is more strained on the surface MgO NS than Al_{14}, because of this

Al_{28}@MgO NS is more stable than Al_{14}@MgO NS. The average surface area to Al_{28}@MgO NS are 7.190 Å, 7.160 Å and Al_{14}@MgO NS are 7.190 Å, 7.176 Å. This means that the structure Al_{28}@MgO NS is less distorted as relative to its peers.

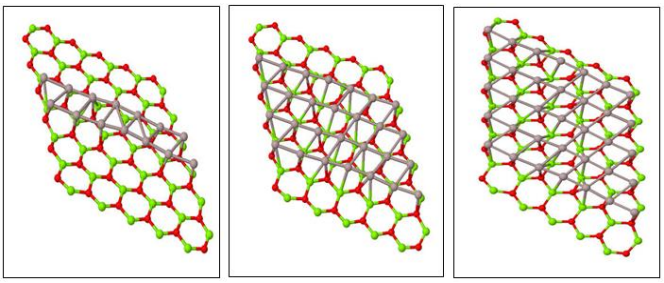

Fig.7: Optimized structures of Al_n@MgONs (n=14, 28, and 35).

Also, variation of binding energy for Al-doped configurations for each doping concentration is represented in **Fig.8**. It is observed that the binding energy decreases with increase in concentration of dopants, indicating the decreasing structural stability as compared to the Al_7@MgONs (E_b = -17.40 eV per atom). This is due to the surface area to MgO NS as well as the nearly similar size of the atomic radius of Al-doped which means there is lesser structural distortion.

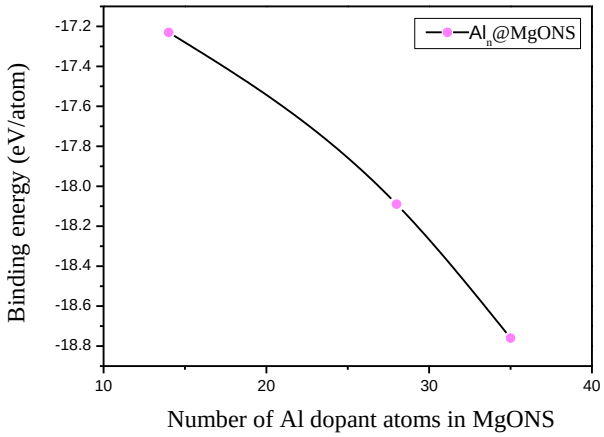

Fig. 8. Variation of binding energy with increasing concentration of Al_n@MgO NS (n=14, 28, and 35) dopants.

The electronic structure analysis shows a narrowing of the band gap for higher dopant concentration, which shows the smallest band gap. A plot of the variation of band gap with doping concentration is shown in **Fig. 9**. Thus Al doping delivers a way to present a gap in MgO NS at the Dirac point to an important value without varying the unique properties of MgO NS.

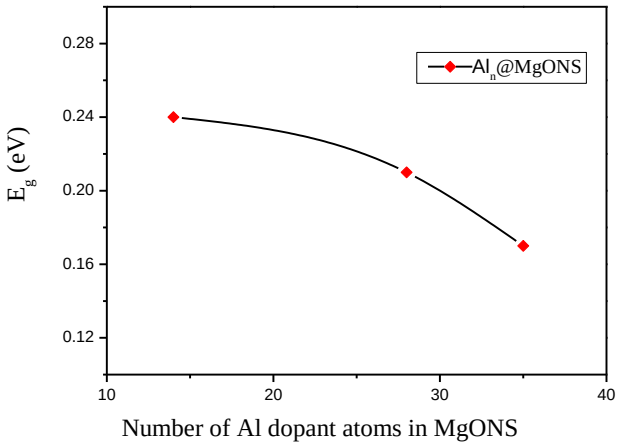

Fig. 9. The band gap with increase in doping concentration of Al_n in MgO NS (n=14, 28, and 35).

On the other hand in **Fig. 10(a)**, the ionization potential is less sensitive and increases exponentially with the increase in the concentration of Al doping to MgO NS structure. This indicates that the ionization potential does not show much dependence on the crystal structure of MgO NS. Also, it is independent of the width of the MgO NS. The structure Al_{35}@MgO NS has higher ionization potential. This means that Al_{28}@MgO NS need large energy to become cation as compared to the other two. **Fig. 10(b)** shows the calculated electron affinity of the structures Aln@MgO NS (n=14, 28, and 35) increasing, That means these structures have a high ability to acceptance electrons and become anions, and in comparison with structure Al_7@MgO NS they are cannot easily to donate an electron to the surrounding species.

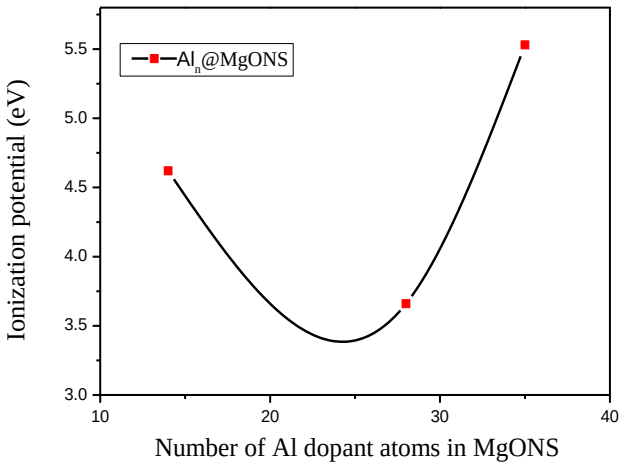

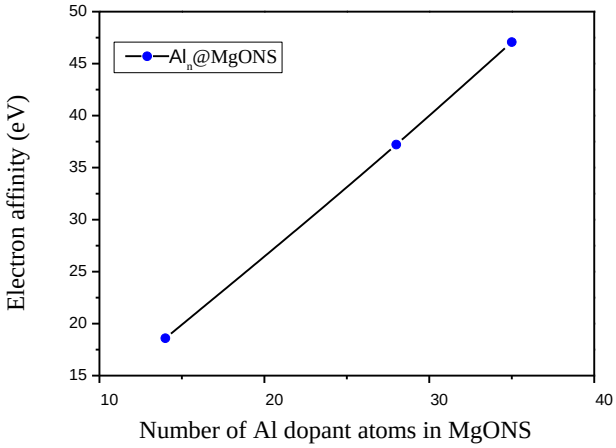

Fig. 10 (a): The ionization potential and (b) electron affinity in increasing order of doping concentrations Al_n@MgO NS (n=14, 28, and 35).

In order to study the influence of dopants on the electronic structures, the electronagtivity indices of Al_n@MgO NS (n=14, 28, and 35) are evaluated and shown in **Fig.11(a)**. It is obvious from the graph that electronagtivity increases as the Al content increases and can be related to the band gap narrowing with increase of the Al concentration. **Fig.11(b)** shows the electrochemical hardness of MgO NS, one can see, hardness decreases with the increase in the concentration of Al doping to the surface area of MgO NS. E_g equals to 0.21eV and 0.17eV. Now, comparing with the structures in the first group, Al_6@MgO NS and Al_7@MgO NS have smaller values of hardness.

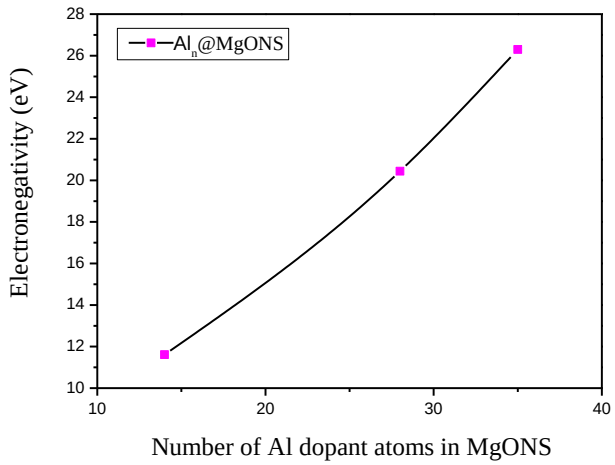

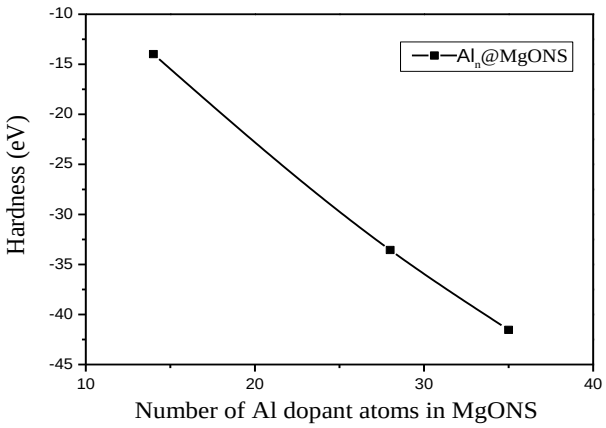

Fig. 11. (a): The electronagtivity and (b) hardness in increasing order of doping concentrations Al_n@MgONs (n=14, 28, and 35).

3.3 Doping of Al_7 and Al_{35} on double layered MgO NS:

In this step, the GGA calculations have been used to obtain optimized structures of two sheets of MgO. As shown in **Fig. 12,** two layers of MgO contain sixty hexagons with the symmetry having the angles in hexagons between 3º to 122.9º[28]. The distance between the two layers are 2.98 Å while two individual Mg–O bonds are distinguished within the layers and another between a hexagon with average bond lengths of 1.88 and 1.95 Å, respectively. This indicates that the structure possesses a real fixed point on surface potential from 120. After that the two layers were doped by exohedral method. In the first case, the two layers were doped with seven Al atoms and the bond length between Al-Mg was kept at about 2.68 Å. In the same manner, two layers were doped with thirty-five atoms of Al.

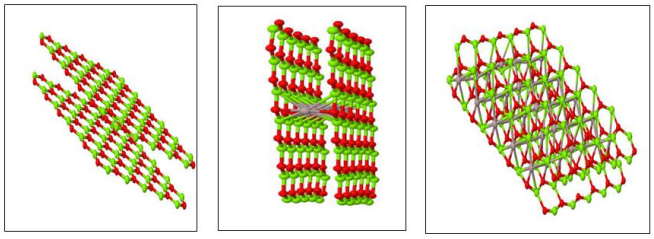

Fig.12: Optimized structures of pure double layered MgO NS and Al_n@MgO NS(n=7 and 35).

We notice that as compared to the binding energy of the system with the one layer, here in this case, it increases by about 2.02 eV for every Mg−O pair

and is more than the mono layer. Also, the binding energies increase with different numbers of doped Al atoms for the double layered MgO NS as shown in **Table 1**. One can see clearly that the band gaps of these doped structures of double layered MgO NSs are smaller than that of single layered MgO NS and strongly depend on number of doped Al atoms[29]. For the case of Al = 7, the band gap is about 0.29 eV and with increasing number of the Al i.e. 35, the band gap increases and comes out to be 0.332 eV. To investigate the electronic properties, we have also calculated ionization potential, electron affinity, electronegativity and hardness of exohedral configurations. Also, we observe the changes in IP & EA with exohedral doping of MgONs as mentioned in Table . The increase in IP& EA with number doping atoms shows the high ability to accept electrons and become anions. The values of EN& H corresponding to n = 7and 35 of Al atoms indicate that they are more reactive with high values of electronegativity EN. All the other structures have smaller values of H in comparison with one layered doped MgO NS. This causes are more soft structure with small excitation energies than the original structure.

Table 1: Calculated Ionization potential (IP) and Electron affinity (AE) Electronegativity (EN) and Hardness (H) in eV for two layer, and Al doped MgONs.

configurations	BE(eV/atom)	E_g (eV)	Ip (eV)	EA (eV)	EN (eV)	H (eV)
2MgONs	-18.420	1.845	3.995	0.850	2.4225	3.145
$Al_7@Mg_{82}O_{82}$	-19.316	0.297	3.351	0.053	1.702	3.298
$Al_{35}@Mg_{82}O_{82}$	-20. 698	0.332	3.411	0.079	1.745	3.332

Conclusions

By using first principles calculations based on DFT, we study the stable structures and electronic properties by exohedral doping of Al atoms on the surface of MgO Ns. We find that Al atoms get adsorbed on flat MgO Ns walkways and monatomic steps, this is because the spin coupling Al-Al bond leads to a net stabilization which is not very affected by the strength of the Al bond during doping. Binding energy, between 16.2 and 17.4 eV for all sites considered corresponds to a metastable. The band gaps for both Al_n@MgO NS NSs exhibit semiconducting properties, having band gaps between 0.45 and 0.20 eV can be significantly tuned by their widths. Al:MgONs systems can be considered as potential material for applications in spintronics, solar energy applications and ultraviolet optielectronic devices.

Acknowledgement

Authors are grateful to the SIESTA group for providing their computational code and the authors would like to express their sincere appreciation to the Department of Physics, Science of college, Kerbala University, Karbala, Iraq.

References

[1] R. Wahab, *et al.*, "Synthesis of magnesium oxide nanoparticles by sol-gel process," in *Materials Science Forum*, 2007, pp. 983-986.

[2] L. Zhang, *et al.*, "MgO nanosheet assemblies supported CoMo catalyst with high activity in hydrodesulfurization of dibenzothiophene," *Industrial & Engineering Chemistry Research*, vol. 54, pp. 5580-5588, 2015.

[3] M. Kiguchi, *et al.*, "Atomic and electronic structure of an unreconstructed polar MgO (111) thin film on Ag (111)," *Physical Review B*, vol. 68, p. 115402, 2003.

[4] R. Arita, *et al.*, "Polar surface engineering in ultrathin MgO (111)⁄ Ag (111): Possibility of a metal-insulator transition and magnetism," *Physical Review B*, vol. 69, p. 235423, 2004.

[5] A. Del Vitto, *et al.*, "Au atoms and dimers on the MgO (100) surface: a DFT study of nucleation at defects," *The Journal of Physical Chemistry B*, vol. 109, pp. 8040-8048, 2005.

[6] K. Zhu, *et al.*, "Efficient preparation and catalytic activity of MgO (111) nanosheets," *Angewandte Chemie International Edition*, vol. 45, pp. 7277-7281, 2006.

[7] A. Akhtar, R. Pilevarshahri, and Mohammad Reza Benam," Investigating and comparison of electronic and optical properties of MgO nanosheet in (100) and (111) structural directions based on the density functional theory" Physica B

502(2016) 61–67.
[8] M. Mantilla, *et al.*, "Oxidation of Mg/Ag (1 1 1) investigated using scanning tunneling microscopy: Towards atomically smooth MgO nanostructures," *Surface science,* vol. 602, pp. 3089-3094, 2008.
[9] K. Matsuzaki, *et al.*, "Layer-by-layer epitaxial growth of polar MgO (111) thin films," *Physical Review B,* vol. 82, p. 033408, 2010.
[10] S. Benedetti, *et al.*, "Competition between polar and nonpolar growth of MgO thin films on Au (111)," *The Journal of Physical Chemistry C,* vol. 115, pp. 23043-23049, 2011.
[11] S. Benedetti, *et al.*, "Chromium-Doped MgO Thin Films: Morphology, Electronic Structure, and Segregation Effects," *The Journal of Physical Chemistry C,* vol. 119, pp. 25469-25475, 2015.
[12] Bromand Nourozia, Amin Aminian, Narges Fili, Yousof Zangeneh, Arash Boochani, and Pezhman Darabi, *Results in Physics*, vol.12, 2038–2043, 2019.
[13] Li-Jie Shi,First-principles prediction of the magnetism of 3d transition-metal-doped Rocksalt MgO, Physics Letters A 374 (2010) 1292–1296
[14] E. Aratch, D. Sanchez-Potral, P. Orejon, A. Garcia, and J. M. Soler, *Phys. Stat. Sol. (b)*, vol. 215, 809,1999.
[15] Nibras Mossa Umran and Ranjan Kumar, *Quantum Matter*, vol4, 1–5, 2015.
[16] J.P. Perdew, K. Burke, M. Ernzerhof, *Phys. Rev.* Lett. vol. 77, 3865, 1996.
[17] Nibras Mossa Umran and Ranjan Kumar, *Physica B*, vol. 437, 47–52, 2014.
[18] Haneen Ali Rashed, Nibras Mossa Umran, *Mater. Res. Express,* vol. 6, 045044, 2019
[19] L. Giordano, *et al.*, "Properties of MgO (100) ultrathin layers on Pd (100): Influence of the metal support," *Physical Review B,* vol. 67, p. 045410, 2003.
[20] J. Goniakowski, *et al.*, "Using polarity for engineering oxide nanostructures: structural phase diagram in free and supported MgO (111) ultrathin films," *Physical review letters,* vol. 93, p. 215702, 2004.
[21] M. Yeganeh and F. B. Baghsiyahi, "Vibrational and Thermodynamical Properties of MgO Nanosheets of (111) and (100) Facets by Density Functional Theory," *Journal of Electronic Materials,* vol. 48, pp. 3816-3822, 2019.
[22] Y. Zhang, *et al.*, "Structural features and electronic properties of MgO nanosheets and nanobelts," *The Journal of Physical Chemistry C,* vol. 116, pp. 23130-23135, 2012.
[23] L. Giordano, *et al.*, "Nucleation of Pd dimers at defect sites of the MgO (100) surface," *Physical review letters,* vol. 92, p. 096105, 2004.
[24] R. M. Martin, *Electronic structure: basic theory and practical methods*: Cambridge university press, 2004.
[25] D. Wu, *et al.*, "Stabilizing graphitic thin films of wurtzite materials by epitaxial strain," *Physical review letters,* vol. 107, p. 236101, 2011.
[26] J. A. Santana, *et al.*, "Structural stability and defect energetics of ZnO from diffusion quantum Monte Carlo," *The Journal of chemical physics,* vol. 142, p. 164705, 2015.
[27] R. Shankar, *et al.*, "Calculation of ionization potential and chemical hardness: A comparative study of different methods," *International Journal of Quantum Chemistry,* vol. 109, pp. 764-771, 2009.
[28] D. A. Abanin, *et al.*, "Spin-filtered edge states and quantum Hall effect in graphene," *Physical review letters,* vol. 96, p. 176803, 2006.
[29] Y.-W. Son, *et al.*, "Energy gaps in graphene nanoribbons," *Physical review letters,* vol. 97, p. 216803, 2006.